Introducing passive matched field acoustic tomography

O. GASPARINI ([1]), C. CAMPOREALE ([1]) and A. CRISE ([2])
([1]) *Dune Srl - Via Tracia 4, Roma, Italy*
([2]) *O.G.S. - Borgo Grotta Gigante, Trieste, Italy*

(ricevuto il 27 Maggio 1996; approvato il 15 Maggio 1997)

Summary. — In acoustic tomography sea-basin environmental parameters such as temperature profiles and current-velocities are derived, when ray propagation models are adopted, by the travel time estimates relative to the identifiable ray paths. The transmitted signals are either single frequency, or impulsive, or intermittent and deterministic. When the wavelength is comparable with the scale lengths present in the propagation scenario, Matched Field Tomography (MFT) is used, entailing the consideration of waveguide modes instead of rays. A new concept in tomography is introduced in the paper, that employs *passively* the noise emitted by ships of opportunity (cargoes, ferries) as source signals. The passive technique is acoustic-pollution-free, and if a basin is selected in which a regular ship traffic occurs data can be received on a regular schedule, with no transmission cost. A novel array pre-processor for passive tomography is introduced, such that the signal structure at the pre-processor output is nearly the same as that obtainable in the case of single-frequency source signals. Hence, at the pre-processor output all the tomographic inversion methods valid for active tomography employing single-frequency sources can be applied. The differences between active and passive tomography are pointed out and the potential of passive techniques is illustrated by simple propagation scenarios adopting either rays or waveguide modes.

PACS 92.10.Mr – Thermohaline structure and circulation.
PACS 43.60 – Acoustical signal processing.

1. – Introduction

Synoptic measurements of environmental parameters such as temperature profiles, currents and fluxes are of paramount oceanographic interest as the open ocean/shelf exchange is influenced by the different spatial and temporal scales of the circulation. The above quantities affect not only the physical, but also the chemical and biological response of the basins.

Acoustic tomography is a valid tool for this task. Single-frequency, impulsive or intermittent deterministic signals are transmitted by fixed or slowly moving sources

and are received by fixed or slowly moving arrays. In classical tomography the basin environmental parameters, such as temperature profiles and sea currents, are derived by the estimates of the *absolute* travel times of the identifiable *ray* paths.

Increasing the wavelength is recommended, in order that the lack of detailed knowledge of the basin at scales smaller than the wavelength has negligible influence on the quality of tomographic estimation. However, the propagation models based on rays are not adequate when the wavelength becomes comparable with the scale lengths present in the propagation scenario. The ray model has also another limitation, as in the presence of multipath the time arrivals relative to the slowest propagating rays (which are important as they are usually associated to the powerful part of the signal, see [1], sect. **1**) become so close that these crowded last rays arrivals cannot be resolved in time.

To overcome the collapsing of the time resolution capability of tomography based on ray models, and to cope with the finite value of the wavelength, coherent propagation models [2]-[6] entailing the consideration of *waveguide modes* have been introduced, which have recently given rise to Matched Field Tomography (MFT) (see [3], sect. **12**), which exploits the full field across receiving arrays with spatially phase-coherent signal processing. The duality of the description of the propagation in terms of rays or of modes has been recognised since the early days of tomography.

While several algorithms for MFT have been proposed, experiments to test them are at a start. The MFT techniques usually employ the same type of source signals as adopted in ray tomography, which are either single-frequency (CW) signals, or wideband impulsive signals, or intermittent signals. Due to the time-dispersive characteristics of the basin, the convenience of employing processing techniques in the spectral domain as a tool of analysis has been recognised.

In the recent years, however, acoustic tomography has been criticised by environmentalist associations because of acoustic pollution on the environment, and specifically on marine mammals. The pressure of environmentalist associations in the USA has halted in 1994 an ambitious project on global tomography in the Pacific Ocean on the basis that it seriously disturbs animal life.

To cope with this difficulty, which is likely to become more serious with time, a new concept in tomography is introduced in this paper, which employs *passively* the noise emitted by ships of opportunity (cargoes, ferries) as source signals for measuring physical oceanographic parameters (temperature profiles, sea currents) in shallow-medium coastal waters (down to a few hundred meter depth).

This technique will be indicated by Passive MFT (P), in contrast with usual tomography (indicated by Active MFT, A) which employs transmitting sources specially conceived for the task of tomography.

Beyond being acoustic-pollution-free, the P technique is interesting because in a basin where ship traffic occurs on a regular schedule plenty of data can be received with no transmission cost, the data set can be sifted to sort out the best conditioned data, etc.

The concept of passive tomography is summarised as follows.

The nominal propagation conditions in the basin, as seen by the measuring points, are assumed as known by preliminary investigations. Variations of sound speed profiles (and then of temperature), modelled parametrically with few parameters as shown in [7], and current velocities, have to be estimated.

The main differences and the additional problems which arise when passing from active to passive tomography are:

– the source signals in P are wideband, stochastic, nearly stationary in the data gathering interval, and of unknown spectra, while in A they are either impulsive, or intermittent, or CW, and they are known, with the possible exception of impulsive signals;

– in P relative motion between sources and receivers is present: motion, when present in A, has demonstrated not to be an impairment [8]-[11]; in P, however, the source motion, not under control of the experimenter, may induce problems more severe than in A;

– in A the relative positions between transmitter(s) and receiver(s) are known. In P we assume that the positions of the ships present in the basin are known, at least approximately: by agreement between the experimenters and the companies operating the ferries and cargoes, ship locations and velocities, derivable for example by GPS onboard the ships, are made available to the experimenters. The case of unknown ship position is also shortly addressed;

– one (or several) array(s) of hydrophones is(are) deployed, whose band is large enough to collect the wideband signals of unknown spectra emitted by the ships.

The concept of passive tomography would be of scarce interest if a methodology for signal processing and tomographic estimation had to be developed anew to cope with the source signals in P, which are different than in A. The point of interest for P is that a novel array pre-processor [12] is available, such that the data structure at the pre-processor output is nearly the same as the one obtainable in the case of CW source signals. Hence at the pre-processor output all the tomographic methods valid for active tomography employing CW sources can be applied. With respect to active tomography employing actual CW source signals, potentially P might have reduced performances due to additional errors in deriving CW (or nearly so) signals by finite-duration data observation intervals, and due to the incompleteness of the observability of the propagation channel achievable by passive means. It is believed that the problem can be handled by suitable array size and enhanced signal processing.

To highlight the differences between A and P and to illustrate in principle the capability of environmental parameter estimation, simple idealised propagation scenarios adopting either rays or waveguide modes will be assumed. References will be quoted, especially in sect. **7**, addressing more complex or actual scenarios.

After the list of symbols (sect. **2**), a short waveguide description of the propagation channel is given in sect. **3**. In sect. **4** the wideband array pre-processor is introduced, followed by matched field tomography for one and several sources (sect. **5**). In sect. **6** the problems introduced by source motion are shortly analysed. In sect. **7** alternative types of tomographic estimators present in the technical literature are indicated. Section **8** describes additional features of the array pre-processor, followed by conclusions in sect. **9**.

2. – List of symbols

$+$	indicates conjugate transposition
$*$	indicates convolution
$\langle\ \rangle$	ensemble average
$\langle\ \rangle_T$	time average over the interval of duration T

$\lvert\cdot\rvert$	amplitude of a complex vector
ω	pulsation
$p = \alpha + j\omega$	variable of the LT
B	source bandwidth
N	number of hydrophone elements of the array
M	number of frequency bins in the source bandwidth
$x_i(t)$	signal emitted by source i, complex envelope
$r_i(\tau) = \langle x_i(t+\tau/2)\, x_i^+(t-\tau/2)\rangle$	autocorrelation of the source (ship) signal i
$g_i(\omega) = FT$	of $r_i(\tau)$ spectral power density of source signal i
$y_j(t)$	complex envelope of the j-th array element output
$h_{ji}(t)$	scalar channel response, mapping $x_i(t)$ into $y_j(t)$
T	duration of the data observation interval
T_c	sampling interval
T_p	propagation delay along the array
B_b	bandwidth of the frequency bin in TC pre-processor
$\mathbf{R}(\tau)$	cross-correlation matrix between array elements at lag τ
$\mathbf{R}_{hk}(\tau) = \langle y_h(t+\tau/2)\, y_k^+(t-\tau/2)\rangle$	element h, k of $\mathbf{R}(\tau)$
$\mathbf{S}(\omega)$	output cross-spectral matrix for pulsation ω: FT of $\mathbf{R}(\tau)$
$\mathbf{H}_i(\omega)$	$\equiv$ array CW vector = FT of the vector $(h_{i,1}^+(t), \ldots, h_{i,N}^+(t))^+$ associated to source i
$H_{ji}(\omega)$	j-th component of vector $\mathbf{H}_i$
$\widetilde{\mathbf{H}}_i(\omega)$	*modelled* array CW vector corresponding to $\mathbf{H}_i(\omega)$
$\mathbf{U}_k(\omega)$	k-th eigenvector of the matrix $S(\omega)$
$\lambda_k(\omega)$	k-th eigenvalue of the matrix $S(\omega)$
c	$c_0 + \Delta c$, sound speed
c_0	nominal value of sound speed
Δc	unknown variation of sound speed
$k = \omega/c$	wavenumber
r_j	range between source and receiving j-th array element
z_1	source depth
z_j	j-th array element depth
ψ	generic value of the depth eigenfunction
ψ_m	depth eigenfunction relative to the m-th mode
Q	no. of propagating modes
ξ	generic value of the range wavenumber (real and positive)
ξ_m	range wavenumber (real and positive) of the m-th mode
$\mathbf{W}$	observation matrix of dimension $N \times Q$, $\mathbf{W}_{jm} = \psi_m(z_j)$
$\varrho(z_1)$	water density at source depth z_1
$\delta(\cdot)$	Dirac's impulse function

FT	Fourier Transform
LT	Laplace Transform
EVD	Eigenvector-eigenValue Decomposition
SVD	Singular Value Decomposition
MFP	Matched Field Processing
CW	Continuous Wave, single frequency signal
P	Passive matched field tomography
A	Active matched field tomography
TC	Transform-and-Correlate technique

CT	Correlate-and-Transform technique
MFT	Matched Field Tomography
MMP	Matched Mode Processing
GPS	Global Positioning System

3. – Waveguide modes

Consider a simple propagation scenario, in which the sound speed $c = c(z)$ depends only on the depth co-ordinate z, and neither on range r nor on azimuth. In this case the Helmholtz equation [3, 4, 6] for the pressure $p(r, z)$ for CW signals is given by

$$\frac{\partial^2 p}{\partial r^2} + \frac{1}{r}\frac{\partial p}{\partial r} + \frac{\partial^2 p}{\partial z^2} + k^2(z)\, p = -\frac{2}{r}\delta(z - z_1)\,\delta(r), \qquad k(z) \equiv \frac{\omega}{c(z)}, \tag{1}$$

with the boundary conditions

$$\begin{cases} p(r, 0) = 0 & \text{(at the air-sea interface)}, \\ \lim_{z \to \infty} p(r, z) = 0 & \text{(radiation condition)} \end{cases} \tag{2}$$

and the local conditions descriptive of the sea-bottom interface. The solution of the homogeneous form of eq. (1) can be found by separating the variables. The wave outgoing from the source has the form (see list of symbols)

$$p(r, z) = H_0^{(1)}(\xi r)\, \psi(z), \tag{3}$$

where $H_0^{(1)}(\xi r)$ is a Hankel function of the first kind of the zero-th order and the depth eigenfunction $\psi(z)$ satisfies the equation

$$\frac{\mathrm{d}^2 \psi}{\mathrm{d}z^2} + [k^2(z) - \xi^2]\, \psi = 0, \tag{4}$$

with proper boundary conditions. We define the depth and range wavenumbers k_z, ξ as

$$k_z^2 \equiv k^2(z) - \xi^2. \tag{5}$$

At distances quite apart from the source, the pressure at the output of the j-th array element, which is the j-th component $H_{j,1}(\omega)$ (see list of symbols) of the array CW vector associated to the source is

$$H_{j,1}(\omega) = \gamma \sum_{m=1}^{Q} \frac{\psi_m(z_1)\, \psi_m(z_j)}{\sqrt{r_j \xi_m}} \exp[\, j\xi_m r_j], \tag{6}$$

where

$$\gamma = j\sqrt{\frac{1}{8\pi}} \exp[-j\pi/4]\, \varrho(z_1). \tag{7}$$

We assume for simplicity of notation a vertical array, and $r_j \cong r$. We define:

Π: diagonal propagation matrix of dimension $Q \times Q$; $\Pi_{mm} = \exp[j\xi_m r](\xi_m r)^{-1/2}$;

$s_m = \Pi_{mm}\psi_m(z_1)$: m-th element of the *modal* source vector **s** of dimension $Q \times 1$.

Equation (6) can be rewritten as follows:

$$\mathbf{H} = \gamma \mathbf{W}\mathbf{s} \,. \tag{8}$$

Equation (8) indicates that the array CW vector is the product of the matrix **W**, which depends only on the basin characteristics at the array location, times the vector **s** which depends on the source emission and on the channel propagation. If the array is not vertical a slight modification of the matrix **W** is required to account for the differential phase across the array.

4. – Wideband array pre-processor

The underwater acoustic channel, whose model assumed linear is given in fig. 1 for two sources, has to be identified by processing the hydrophone array output signals $y_j(t)$. The noise sources due to the two ships are stochastic, wideband, stationary, ergodic and mutually independent.

Assume for the moment that only source 1 is present, in the absence of additive noise. We have

$$y_k(t) = \int h_{k,1}(t)\, x_1(t-\sigma)\, \mathrm{d}\sigma \,. \tag{9}$$

The element h, k of the output cross-correlation matrix at lag τ is estimated by time averaging in a data observation interval having duration T

$$\left\langle y_h\left(t+\frac{\tau}{2}\right) y_k^{+}\left(t-\frac{\tau}{2}\right)\right\rangle_T = \tag{10}$$

$$= \int\int h_{h,1}(\sigma)\, h_{k,1}^{+}(\lambda) \left\langle x_1\left(t+\frac{\tau}{2}-\sigma\right) x_1^{+}\left(t-\frac{\tau}{2}-\lambda\right)\right\rangle_T \mathrm{d}\sigma\, \mathrm{d}\lambda \,.$$

Assuming that stationarity and ergodicity hold in the interval, and that $BT \gg 1$, we have (see list of symbols)

$$\left\langle x_1\left(t+\frac{\tau}{2}-\sigma\right) x_1^{+}\left(t-\frac{\tau}{2}-\lambda\right)\right\rangle_T \cong \tag{11}$$

$$\cong \left\langle x_1\left(t+\frac{\tau}{2}-\sigma\right) x_1^{+}\left(t-\frac{\tau}{2}-\lambda\right)\right\rangle = r_1(\tau+\lambda-\sigma),$$

$$R_{hk}(\tau) = \left\langle \mathbf{y}_h\left(t+\frac{\tau}{2}\right) \mathbf{y}_k^{+}\left(t-\frac{\tau}{2}\right)\right\rangle = \int\int h_{h,1}(\sigma)\, h_{k,1}^{+}(\lambda)\, r_1(\tau+\lambda-\sigma)\, \mathrm{d}\sigma\, \mathrm{d}\lambda \,. \tag{12}$$

By taking FT of eq. (12) with respect to lag τ, we get

$$S_{hk}(\omega) \equiv \int R_{hk}(\tau)\, \mathrm{e}^{-j\omega\tau}\, \mathrm{d}\tau = \int\int h_{h,1}(\sigma)\, h_{k,1}^{+}(\lambda)\, \mathrm{d}\sigma\, \mathrm{d}\lambda \int r_1(\tau+\lambda-\sigma)\, \mathrm{e}^{-j\omega\tau}\, \mathrm{d}\tau \,. \tag{13}$$

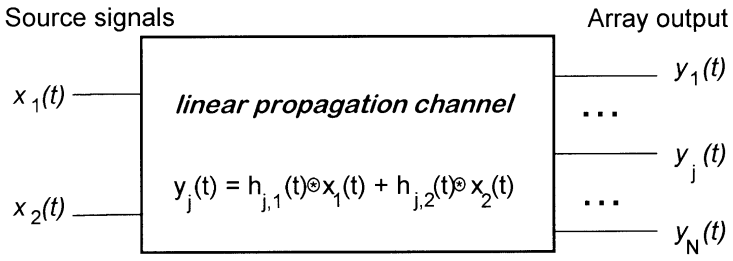

Fig. 1. – Input-output description of a linear propagation channel.

Since

$$g_1(\omega) \equiv \int r_1(\tau)\, e^{-j\omega\tau}\, \mathrm{d}\tau\,, \tag{14}$$

hence

$$\int r_1(\tau + \lambda - \sigma)\, e^{-j\omega\tau}\, \mathrm{d}\tau = g_1(\omega)\, e^{j\omega(\lambda - \sigma)}. \tag{15}$$

By combining eqs. (13) and (15) the element h, k of the output cross-spectral matrix $\mathbf{S}(\omega)$ is derived:

$$S_{hk}(\omega) = g_1(\omega) \int\int h_{h,\,1}(\sigma)\, h^{+}_{k,\,1}(\lambda)\, e^{j\omega(\lambda - \sigma)}\, \mathrm{d}\sigma\, \mathrm{d}\lambda = \tag{16}$$

$$= g_1(\omega) \Big[\int h_{h,\,1}(\sigma)\, e^{-j\omega\sigma}\, \mathrm{d}\sigma \Big] \Big[\int h_{k,\,1}(\lambda)\, e^{-j\omega\lambda}\, \mathrm{d}\lambda \Big]^{+}.$$

Hence the following matrix equation is valid:

$$\mathbf{S}(\omega) = g_1(\omega)\, \mathbf{H}_1(\omega)\, \mathbf{H}_1^{+}(\omega)\,, \tag{17}$$

in which the output cross-spectral matrix is proportional to the outer product of the array CW vector $\mathbf{H}_1(\omega)$ by itself.

In the case of two mutually independent sources, we have

$$\mathbf{S}(\omega) = g_1(\omega)\, \mathbf{H}_1(\omega)\, \mathbf{H}_1^{+}(\omega) + g_2(\omega)\, \mathbf{H}_2(\omega)\, \mathbf{H}_2^{+}(\omega)\,. \tag{18}$$

The equations above are valid for any value of bandwidth, any wavefront shape and any array geometry.

We will assume that $|\mathbf{H}_i(w)| = 1$; for the remaining part of this section the one-source case will be analysed.

By taking an Eigenvector-eigenValue Decomposition (EVD) of the output cross-spectral matrix at the left-hand side of eq. (17), the first eigenvector $\mathbf{U}_1(\omega)$ is obtained, which is related to $\mathbf{H}_1(\omega)$ as follows:

$$\mathbf{H}_1(\omega) = \varphi_1(\omega)\,\mathbf{U}_1(\omega), \qquad |\varphi_1(\omega)| = 1, \qquad |\mathbf{U}_1(\omega)| = 1, \tag{19}$$

where $\varphi_1(\omega)$ is a unit-amplitude (phase-only) scalar function which cannot be determined by the eigenvector decomposition of the cross-spectral matrix. Hence from the EVD of the output cross-spectral matrix the array CW vector $\mathbf{H}_1(\omega)$ is obtained, apart from a phase-only term which multiplies each vector component. We will assume for sake of simplicity that $\varphi = 1$, so that $\mathbf{H}_1(\omega) = \mathbf{U}_1(\omega)$.

Suppose now that the source signal is CW, and is given by $\exp[j\omega t]$; it can be verified immediately that the array output vector signal is $\exp[j\omega t]\,\mathbf{H}_1(\omega)$. So, the array CW vector $\mathbf{H}_1(\omega)$ which in the case of a wideband stochastic source can be derived by the eigendecomposition of the cross-spectral matrix, is identical, apart from a phase-only scalar factor, to the time output signal valid for a CW source.

A large body of techniques is available for CW source signals both for channel modelling and tomographic inversion. Since in the presence of ship-generated noise the signals are not CW, but stochastic and wideband, the array CW vector for a generic value of frequency in the band is estimated (apart from a phase-only scalar factor) by the technique indicated above in which Correlation is followed by Fourier Transform (this technique will be indicated as CT). After this pre-processing step *all* the inversion methods valid for CW sources can be employed.

In practice, since the sources are ergodic, the cross-correlation matrix *vs.* lag is estimated by the data observed in an interval of finite duration. In this paper the values of the averages will be assumed identical to the ensemble averages.

To illustrate the issue of channel parameter estimation, three simple examples will be examined, in which idealised propagation *ray* models are assumed.

Example 1

In fig. 2 (neglecting the reflected path) a simple scenario is indicated in which a planar wave from source (1) impinges on a vertical linear array. The array CW vector in correspondence to a signal $\exp[j\omega t]$ can be derived by inspection from the figure:

$$H_{k,1}(\omega) = \frac{1}{\sqrt{N}} \exp\left[j\omega\left[t - \frac{r}{c}\right]\right] \exp\left[-j\omega\,\frac{D_k}{c}\sin\theta_1\right], \tag{20}$$

where r is the distance between the source and the first array element, and D_k the distance between the first and the k-th array element ($D_1 = 0$).

In the common scalar factor at the right member of eq. (20), information on the distance r between the source and the array and on the value of the sound speed in the channel between source and array are present. However, this scalar cannot be determined by EVD of the cross-spectral matrix. This indicates simply that when passing from active to passive channel identification an *absolute* propagation delay between the source and an array element cannot be determined by passive means, and that channel observability is incomplete; only *relative* propagation delays between array elements can be estimated.

Assume that the ship position is known via GPS, and that the value of θ_1 can be determined by knowing the channel and the array geometry. Since the sound speed c

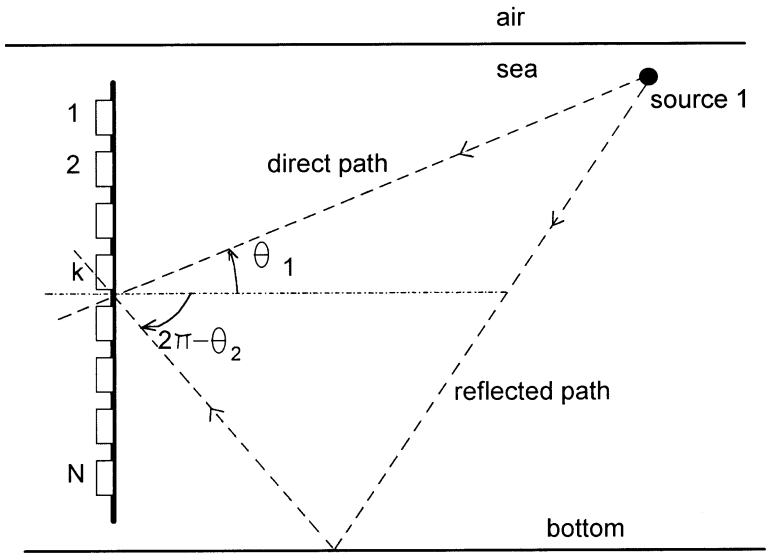

Fig. 2. – Propagation scenario with a signal source, a receiving array and two rays.

which appears in the vector components of eq. (20) (omitting the common factor) pertains to a small portion of the channel, which is the one including the interelement paths, its identification would bear no information on the sound speed variation relative to the channel comprised between the source and the array.

Example 2

A more interesting idealised scenario is depicted in fig. 2, considering both paths. We have now, omitting the (positive) vector normalisation factor,

$$H_{k,1}(\omega) = \frac{1}{1+A}\exp\left[j\omega\left[t-\frac{r}{c}\right]\right]\cdot \cdot\left[\exp\left[-j\omega\frac{D_k}{c}\sin\theta_1\right]+A\exp\left[-j\omega\frac{D_k}{c}\sin\theta_2\right]\right]. \tag{21}$$

The quantity A is a complex factor including information on the propagation delay between the direct and reflected paths and the reflection modality at the bottom:

$$A = A_0\exp\left[-j\omega\frac{\Delta r}{c}\right], \tag{22}$$

where $\Delta r = r_r - r$ is the difference between the reflected r_r and the direct path, r. By

omitting the common exponential factor, we can re-write eq. (21) as follows:

$$(23)\qquad \begin{cases} H_{11}(\omega) = 1\,, \\ H_{k,1}(\omega) = \exp\left[-j\omega\,\dfrac{D_k}{c}\sin\theta_2\right] + \\ \qquad\qquad + \dfrac{1}{1+A}\left[\exp\left[-j\omega\,\dfrac{D_k}{c}\sin\theta_1\right] - \exp\left[-j\omega\,\dfrac{D_k}{c}\sin\theta_2\right]\right]. \end{cases}$$

Equation (23) indicates that the two wavefronts relative to the two paths interfere along the array as far as $\theta_1 \neq \theta_2$. The interference pattern depends on A, which contains information on sound speed relative to the whole channel. An appreciable interference pattern occurs if $|A|$ is comprised in the range $[0.1, 10.]$.

Hence, exploiting the interference pattern along the array provides the potential for estimating the sound speed variation in the whole channel. This potential exists only for those scenarios in which at least two rays associated to two different paths interfere on the array.

Example 3

In a more realistic scenario a number q of widely separated receiving arrays delimit a convex zone in which tomographic estimation has to be performed. Assume that the source signal is emitted by a ship cruising externally to the zone. If each array contains only one element, the statistics of interest is the cross-correlation matrix between elements at lag τ, which contains indications on the acoustical transit time across the elements in correspondence to the source signal, and hence contains information on the basin environmental parameters.

It is questionable which type of statistics should be considered when each array has more than one element. For any two arrays the statistics could be the cross-correlation matrix at lag τ, taken between elements *of the first and of the second array*. Since the ship position is known, the acoustical transit time between the two arrays is approximately known and so is the range of values of τ for which the cross-correlation matrix is non-negligible. After FT of the cross-correlation matrix the resulting matrix is not Hermitian, so SVD (and not EVD) is the proper decomposition to obtain array CW (left and right) vectors. Multiple sources and receivers are required to map complex basin structures, such as range-dependent eddies ([13], fig. 4). The presence of multiple sources, even though not at the same time, can be provided by selecting a basin with a moderate ship traffic.

5. – Matched field tomography

We assume that the ship position is known by GPS, and that the modelled array CW vector is known as a function of the sound speed variation Δc (see list of symbols), which is the only quantity to be estimated. Once the *actual* channel vector is estimated

by EVD, we form the statistics $F(\Delta c)$ to obtain the estimate of Δc

$$F(\Delta c) \equiv \frac{1}{1 - \frac{1}{M} \sum_{k=1}^{M} |\widetilde{\mathbf{H}}_1^{+}(\omega_k)\, \mathbf{H}_1(\omega_k)|^2}, \tag{24}$$

$$\mathrm{Est}(\Delta c) \Leftrightarrow \underset{\Delta c}{\mathrm{Max}}\, F(\Delta c). \tag{25}$$

The integer M indicates a convenient number of selected frequencies comprised in the source band. The source bandwidth can be estimated by plotting the first *eigenvalue* $g_1(\omega)$ of the cross-spectral matrix *vs.* frequency.

Equation (24) has the following meaning:

– The set of normalised vectors $\mathbf{H}_1(\omega_i)$ is derived by performing the EVD of the estimated cross-spectral matrix, at various frequencies, apart from a unit-amplitude phase-only scalar function.

– The presence of a norm in eq. (24) justifies that the phase-only term φ in eq. (19) is set to 1.

– The normalised vectors $\widetilde{\mathbf{H}}_1(\omega_i)$ are function of the sound speed variation Δc; an *a priori* knowledge of the basin structure is required, so that the vector signal arriving at the array, corresponding to a hypothetical CW source, can be modelled as a function of the source position, frequency and channel parameters to be estimated. In the process of searching the estimator peak, the value Δc is varied about the nominal value c_0. The choice of a nominal value is a convenient starting point for the process of estimation of the sound speed variation. When a database of sea measurement is available, the nominal value and the parametrized sound speed variation can be derived as indicated in [7]. Note that the search domain for Δc is small since only *local* variations of sound velocities are considered.

– In the absence of estimation errors, at each frequency the modelled vector $\widetilde{\mathbf{H}}_1(\omega_i)$ and the estimated vector $\mathbf{H}_1(\omega_i)$ coincide in correspondence to the actual value of the sound speed. For this value the inner product $\widetilde{\mathbf{H}}_1^{+}(\omega)\, \mathbf{H}_1(\omega)$ is one, the denominator in eq. (24) is zero and the function $F(\Delta c)$ has a peak of unbounded value. In the presence of noise and of errors in estimating the correlation matrix and in modelling, the estimate of the sound speed variation is still obtained in correspondence to the absolute maximum of eq. (24), which has now a bounded value.

– The ship location is considered approximately known. If the knowledge of the source position is not sufficiently accurate, both the modelled sound speed parameters and the ship position parameters are varied in a domain, in the process of searching the best vector alignment.

Due to the oscillatory nature of the inner products between vectors in eq. (24), spurious secondary maxima might occur for eq. (24) in correspondence to incorrect values Δc, unless proper processing steps are provided. An important step is selecting a proper *space-frequency* grid, which is a set of unevenly spaced array interelement distances and frequencies, so that periodicities are smeared out, and a valid peak is likely to occur only in the presence of the actual value of the sound speed variation. Equation (22) indicates that since the two-path difference Δr can be significant, the

phase of A can be much greater than 2π, so the interference pattern varies significantly by varying the sound speed or the frequency.

5˙1. *Case of several sources.* – Concerning eq. (18), we know the current values of the following quantities:

– The left-hand side member, estimated by the CT technique.

– An estimate of the *number* of the sources: taking the EVD decomposition of the cross-spectral matrix, the number of non-zero eigenvalues is equal to the number of the sources. By indicating with $\lambda_1(\omega)$ the greatest eigenvalue, the following relationship is valid:

$$\lambda_1(\omega) \geqslant \mathrm{Max}\{g_1(\omega), g_2(\omega)\} \geqslant \mathrm{Min}\{g_1(\omega), g_2(\omega)\} \geqslant \lambda_2(\omega). \tag{26}$$

When estimation or additive noise errors are present, the eigenvalues $\lambda_i(\omega)$ for ($i = 3, 4, \ldots, N$) will be small but not zero.

– The vectors $\widetilde{\mathbf{H}}_1(\omega_i)$ derivable by channel modelling and GPS information relative to the two sources.

Note that in eq. (18) only the left member is known, but not the individual quantities $g_i(\omega)$, $\mathbf{H}_i(\omega)$, which appear at the right member.

Two distinct velocity variations Δc_i, $i = 1, 2$ relative to the two channels between each source and the array can be assumed. A channel estimator is indicated below:

$$F(\Delta c_1, \Delta c_2) \equiv \frac{1}{\sum_{k=1}^{M} [\widetilde{\mathbf{H}}_1^+(\omega_k)\, \mathbf{N}(\omega_k)\, \widetilde{\mathbf{H}}_1(\omega_k) + \widetilde{\mathbf{H}}_2^+(\omega_k)\, \mathbf{N}(\omega_k)\, \widetilde{\mathbf{H}}_2(\omega_k)]}, \tag{27}$$

$$\mathrm{Est}(\Delta c_1, \Delta c_2) \Leftrightarrow \underset{\Delta c_1, \Delta c_2}{\mathrm{Max}}\, F(\Delta c_1, \Delta c_2), \tag{28}$$

where $\mathbf{N}(\omega_k)$ is the noise subspace matrix derived by the EVD of the cross-spectral matrix $\mathbf{S}(\omega_k)$:

$$\mathbf{N}(\omega_k) \equiv \sum_{i=3}^{N} \mathbf{U}_i(\omega_k)\, \mathbf{U}_i^+(\omega_k). \tag{29}$$

Equations (27)-(29) are employed to estimate the sound velocity variations in the two channels. The estimator in eq. (27) is a *MUSIC-like incoherent* estimator [14]: as the noise subspace and the subspace spanned by the two source vectors are orthogonal, when the modelled vectors are equal to the actual vectors a peak of the left member of eq. (27) occurs.

In [3] an exhaustive set of estimators for Matched Field Processing (MFP) is reviewed. The MFP technique concerns the processing performed on the array output to estimate source positions when they are unknown, and (possibly) basin parameters. The MFT, in which only basin parameters are estimated, is a particular branch of MFP. Since the aim of this paper is not to review the estimators, the reader should refer to [3].

The estimation procedure is valid also when more than two sources of positions approximately known (by GPS) are present (in this case the lower index in the sum in eq. (29) is set equal to the number of sources plus one). Since the search procedure in a space of higher dimensionality (Δc_1, Δc_2, Δc_3, ...) is involved, and since the likelihood

that estimation errors relative to one channel affect the estimation in the other channels increases, it seems advisable to limit MFT to cases in which a small number of sources are present at the same time.

Assume now that two sources are present, and that the position of the first source is known by GPS, while the position of the second is totally unknown. This may occur when a non co-operative ship is present in the basin. The *number* of ships in the basin can still be detected since it is equal to the number of the dominant spectral eigenvalues of the cross-spectral matrix.

In this case we can still adopt the estimation procedure indicated by eqs. (27), right-hand side, and (29), but in the search space *position parameters* relative to the second source must be included too. Now the search space has an increased dimensionality and the search domain relative to the second source position is a wide one, so the search process does not entail only local variations as in the case of sources of known positions.

Due to the much enlarged size of the search domain, the estimator might lock on spurious maxima. The problem of simultaneous estimation of position and of the environmental parameters has been investigated in the case of active MFT (the problem is referred to as focalisation) [15]. Since acoustic fields are more sensitive to variations in source locations than in environmental parameters, the processor may lock on the correct source location but on wrong environmental parameters.

For this reason, and since it is likely that there will be no shortage of data from scenarios in which a few ships of known (or approximately so) positions are present, it will be advisable to limit the estimation of environmental parameters to scenarios having few sources of known positions.

6. – Source motion and sea currents

In fig. 3, a simple scenario is depicted in which a source and a receiver are at the same depth. We assume that the ship travels toward the receiver with a constant speed v. We indicate by $x(t')$ the wideband stochastic signal emitted by the source at instant t'. A ray time-signal at the receiver associated to the reflected path is proportional to the transmitted signal if the first is measured at an *observation* (or *retarded* [16]) time t, which is related to t' as follows:

$$t = t' + \left(\frac{r_0 - vt'}{\cos\theta} \right) \left(\frac{1}{c + u\cos\theta} \right), \tag{30}$$

$$\tan[\theta(t')] = \frac{2H}{r_0 - vt'}, \tag{31}$$

where

v: ship speed

u: current velocity, assumed horizontal

$r(t') = r_0 - vt'$ distance between source and receiver at instant t'

$c + u\cos\theta$ sound propagation speed along the reflected path.

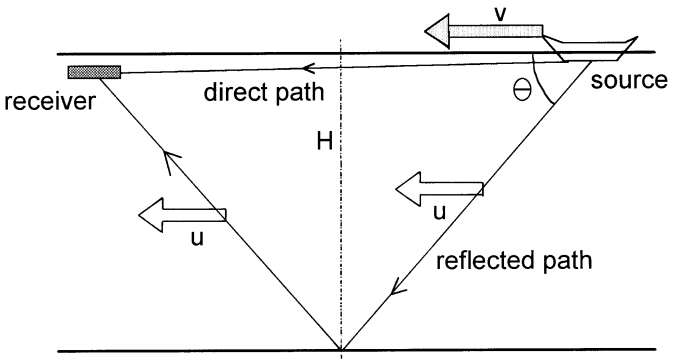

Fig. 3. – Propagation scenario with a moving source, a receiver, sea currents and two rays.

The value of u is positive if the current velocity points to the receiver. From eq. (30) we derive

$$(32)\qquad t' = t\left[1 + \frac{v}{c\cos\theta}\,\frac{1}{1 + \dfrac{u}{c}\cos\theta - \dfrac{v}{c}\,\dfrac{1}{\cos\theta}}\right] - \left(\frac{r_0}{c\cos\theta}\right)\left(\frac{1}{1 + \dfrac{u}{c}\cos\theta - \dfrac{v}{c}\,\dfrac{1}{\cos\theta}}\right) \equiv (1+\alpha)\,t - \beta\,.$$

The signal at the receiver is $x(t') = x[(1+\alpha)\,t - \beta]$. The quantities α, β indicate the variation of the receiver time scale, and the propagation delay between source and receiver. We will assume that α, β do not change appreciably in the data observation interval of duration T.

Consider the difference between the propagation delays for the two paths, the direct path ($\theta = 0$) and the reflected path ($\theta \neq 0$). We have:

$$(33)\qquad \beta(\theta \neq 0) - \beta(\theta = 0) = \frac{r_0}{c}\left[\frac{1}{\cos\theta}\,\frac{1}{1 + \dfrac{u}{c}\cos\theta - \dfrac{v}{c}\,\dfrac{1}{\cos\theta}} - \frac{1}{1 + \dfrac{u}{c} - \dfrac{v}{c}}\right].$$

The functional form of eq. (33) indicates that in principle the variation of the sound speed, the current velocity, and the ship speed can be individually estimated by the pattern of the interference on the array due to several rays (see sect. **4**, example 2). This would not be possible if, for example, in the equation above the quantities u, c, v appear in combinations like $c + u$, or $c + v$, or $u + v$.

6˙1. *Doppler effect.* – We assume that the ship velocity is approximately known together with GPS data.

For the sake of explanation, consider Q rays arriving at the array. The signal $y_h(t)$ at the h-th array element is given by

$$y_h(t) = \sum_{i=1}^{Q} x_1[(1+\alpha_{ih})\,t - \beta_{ih}]. \tag{34}$$

The first and second index at the right-hand side refer to the ray and to the array element, respectively. Equation (32) indicates the value of α, β for the configuration in fig. 3.

Let the source signal be given by

$$x_1(t') = s(t')\exp[j\omega_0 t'], \tag{35}$$

where $s(t')$ is a complex baseband envelope, and ω_0 the *centre pulsation*. We can write

$$y_h(t) = \sum_{i=1}^{Q} s[(1+\alpha_{ih})\,t - \beta_{ih}]\exp[j\omega_0[(1+\alpha_{ih})\,t - \beta_{ih}]]. \tag{36}$$

We simplify the analysis by neglecting α_{ih} in the argument of the complex envelope (but not in the complex exponential). This assumption, although unrealistic since the percentage bandwidth of the source signal is not small, is taken here to point out the kind of problems arising in the presence of source motion.

Now the *ensemble* averages (indicated by the brackets $\langle\cdot\rangle$) of the cross-correlation matrix between sensors is estimated by *time* averaging (indicated by the brackets $\langle\cdot\rangle_T$) in the observation interval. A deterministic *Doppler-demodulating* function $\exp[-jd\omega_0 t]$ is introduced which multiplies all the cross-correlation products and whose aim will be clarified in the following. The h, k element of the cross-correlation matrix is

$$\left\langle y_h\left(t+\frac{\tau}{2}\right) y_k^{+}\left(t-\frac{\tau}{2}\right)\exp[-j\omega_0 dt]\right\rangle_T = \tag{37}$$

$$= \sum_{i=1}^{Q}\sum_{j=1}^{Q}\left\langle s\left(t+\frac{\tau}{2}-\beta_{ih}\right) s^{+}\left(t-\frac{\tau}{2}-\beta_{jk}\right)\exp\left[j\omega_0\left[(1+\alpha_{ih})\left(t+\frac{\tau}{2}\right)-\beta_{ih}\right]\right]\cdot\right.$$

$$\left.\cdot\exp\left[-j\omega_0\left[(1+\alpha_{jk})\left(t-\frac{\tau}{2}\right)-\beta_{jk}\right]\right]\exp[-j\omega_0 dt]\right\rangle_T.$$

We have

$$\left\langle y_h\left(t+\frac{\tau}{2}\right) y_k^{+}\left(t-\frac{\tau}{2}\right)\exp[-j\omega_0 dt]\right\rangle_T = \tag{38}$$

$$= \sum_{i=1}^{Q}\sum_{j=1}^{Q}\left\langle s\left(t+\frac{\tau}{2}-\beta_{ih}\right) s^{+}\left(t-\frac{\tau}{2}-\beta_{jk}\right)\exp[j\omega_0 t[(\alpha_{ih}-\alpha_{jk})-d]]\right\rangle_T\cdot$$

$$\cdot\exp\left[j\omega_0\left[\tau\left(1+\frac{\alpha_{ih}+\alpha_{jk}}{2}\right)-(\beta_{ih}-\beta_{jk})\right]\right].$$

We can write

$$(39)\qquad s\left(t+\frac{\tau}{2}-\beta_{ih}\right)s^{+}\left(t-\frac{\tau}{2}-\beta_{jk}\right)=\left\langle s\left(t+\frac{\tau}{2}-\beta_{ih}\right)s^{+}\left(t-\frac{\tau}{2}-\beta_{jk}\right)\right\rangle+fl(t)\,.$$

The first member is the sum of an *ensemble* average and of a fluctuating part $fl(t)$ having zero average.

Neglecting for the moment the fluctuating part, taking the FT of eq. (38) with respect to τ, taking into account eq. (35) and the definition of $g_1(\omega)$ in the list of symbols, we get an estimate of the h, k element of the *modified* cross-spectral matrix $S_d(\omega)$:

$$(40)\qquad \mathrm{FT}\left\{\left\langle y_h\left(t+\frac{\tau}{2}\right)y_k^{+}\left(t-\frac{\tau}{2}\right)\exp\left[-j\omega_0 dt\right]\right\rangle_T\right\}=$$

$$=\sum_i\sum_j\left[\exp\left[-j\omega\beta_{ih}\exp\left[j\omega_0\beta_{ih}\frac{\alpha_{ih}}{2}\right]\right]\right]\cdot$$

$$\cdot\left[\exp\left[j\frac{\omega_0}{2}(\beta_{ih}\alpha_{jk}-\beta_{jk}\alpha_{ih})\right]\right]\left[\exp\left[-j\omega\beta_{jk}\exp\left[j\omega_0\beta_{jk}\frac{\alpha_{jk}}{2}\right]\right]\right]^{+}\cdot$$

$$\cdot g_1\left[\omega-\omega_0\frac{(\alpha_{ih}+\alpha_{jk})}{2}\right]\left\langle\exp\left[i\omega_0 t[(\alpha_{ih}-\alpha_{jk})-d]\right]\right\rangle_T.$$

In the absence of ship motion and by assuming $d=0$, eq. (40) reduces to

$$(41)\qquad \mathrm{FT}\left\{\left\langle y_h\left(t+\frac{\tau}{2}\right)y_k^{+}\left(t-\frac{\tau}{2}\right)\right\rangle_T\right\}\cong\mathrm{FT}\left\{\left\langle y_h\left(t+\frac{\tau}{2}\right)y_k^{+}\left(t-\frac{\tau}{2}\right)\right\rangle\right\}=$$

$$=g_1(\omega)\left(\sum_i\exp\left[-j\omega\beta_{ih}\right]\right)\left(\sum_j\exp\left[-j\omega\beta_{jk}\right]\right)=g_1(\omega)\,H_{h,1}(\omega)\,H_{k,1}^{+}(\omega)=S_{h,k}(\omega)\,.$$

In this case the unmodified, usual cross-spectral matrix is the outer product of a array CW vector by itself, as indicated in eq. (17), and simple processors based on vector alignment (see eq. (24)) can be employed for the tomographic estimation.

In the case of motion we can assume

$$(42)\qquad g_1\left[\omega-\omega_0\frac{(\alpha_{ih}+\alpha_{jk})}{2}\right]\cong g_1(\omega)\,.$$

The second member of eq. (40), due to the presence of the second factor in square brackets and to the time average, does not factorise in the product of two sums relative to the rays as in eq. (41). The cross-spectral matrix is not the outer product of a source vector by itself, and in general the matrix has a full rank.

Since the distance between source and receiver is much greater than the array length, we can assume $\alpha_{ik}\approx\alpha_i$, so the value α_i depends only on the i-th mode and not on the array element. The quantities α_i, α_j have the same sign and for modes having near indices we have

$$(43)\qquad |\alpha_i-\alpha_j|\ll\mathrm{Min}\{|\alpha_i|,\,|\alpha_j|\}\,.$$

Now, corresponding to the values of $i = i_0$, $j = j_0$, we assume $\delta = a_{i0} - \alpha_{j0}$ to compensate the phase rotation due to the Doppler frequency. For this pair of modes the time-average in the last factor at the right-hand side of eq. (40) is equal to one, while for the other pairs the averages are smaller than one. By taking in turn different values of δ to compensate the phase rotation due to different couples of modes, a set of cross-spectral matrices is obtained in which the contributions of distinct couples of modes are highlighted in turn.

Yet, the second member of eq. (40) cannot be factorized into two sums, as the second (cross-coupling) factor is still present, and a simple processor based on vector alignment cannot be employed. A naive estimation criterion might be that based on the similarity of the set of estimated Doppler-compensated spectral matrices with the homologous modelled matrices. Another criterion might be to process directly the cross-correlation matrix between array elements taken at various lags, the inversion process consisting in achieving the match between a predicted cross-correlation matrix and a measured one.

The influence of the fluctuating part in eq. (39) is now shortly examined. If the product BT is much greater than one, for the couple of rays for which the Doppler rotation is compensated the contribution of the fluctuating part $fl(t)$ after time average becomes negligible with respect to the contribution of the ensemble average. For those couples of modes for which Doppler rotation is not compensated, a contribution of the fluctuating part will occur in correspondence to the frequencies around the *uncompensated* Doppler, $\omega_0[(\alpha_{ih} - \alpha_{jk}) - \delta]$.

When the factors α_{ih} cannot be neglected in the complex baseband envelope (eq. (36)), the processing will entail re-alignment of the time scales of pairs of received signals before estimating the correlation products.

The simple ideas presented so far could be developed to assess the influence of motion, and to synthesise suitable tomographic estimators. The circumstance that the α_i coefficients are much smaller than one will have to be exploited to ascertain whether the estimators can be derived by perturbation techniques from the zero Doppler estimators.

The problem of Doppler compensation arises also in the case of active tomography with towed sources [8-11]. The circumstance that in the active case the Doppler is not a serious impairment gives a hint that the problem can be coped with also in the present case.

7. – Alternative tomographic estimators

The estimation method indicated so far (eqs. (24), (27)) which is based on alignment between estimated and modelled array CW vectors, is indicated as *beamforming*. Estimation methods other than beamforming can be employed.

– In [1, 7, 17], the propagation delays of the waveguide modes are estimated first by frequency-domain techniques, then the delays are processed for tomographic inversion. Although the last step resembles the one adopted in classical tomography based on ray path travel times, the intermediate processing step in the frequency domain exploits the channel coherence to resolve time delays unresolvable via classical ray tomography. In [18] ray and mode travel times and their perturbations are assessed for achieving *internal wave tomography*: a discrepancy is found since modal and ray travel time variances due to internal waves result substantially different for

rays and modes at the same grazing angle. In [19] the ray and mode travel time variances are thoroughly analysed and the discrepancy is eliminated.

– In [3], eq. (67), and in [13, 17], the estimated phases of the waveguide modes are employed as the basic statistics for tomographic inversion.

– Matched Mode Processing (MMP) [3, 20-23] is a recent technique based on eq. (8): after estimating the array CW vector an estimate of the modal source vector **s** is obtained by inverting, or pseudo-inverting eq. (8). The modal source vector, which contains information on the basin parameters, is the basic statistics employed for tomographic inversion. In MFP and MFT the basic statistics for inversion, consisting in the array CW vectors, concerns the array space, while in MMP the statistics concerns the mode space. The potential advantage of MMP is the following: high-order modes, which generally couple to the boundary, are less predictable and this may introduce uncertainty in the modelled CW vector. In MMP a number of modes smaller than the number Q of propagating modes can be selected before forming the statistics for inversion: ruling out high-order modes allows control of the environment matching. This is a distinct advantage on MFT, in which all the propagating modes are present in the basic statistics used for inversion. However, the array geometries and the signal-to-noise ratio required by MMP appear formidable [3].

Deriving environmental parameters from the estimated travel times relative to ray or modes may introduce mathematical difficulties because the unknown sound speed appears nonlinearly in the modelled channel response [7]. A feature of interest in MFT based on beamforming is that the estimation is based on the matching of the spatial structure of the observation with modelled responses rather than on inversion operating on some derived parameters, such as travel times; even if the sound speed variation appears in whatsoever complicated nonlinear function in the modelled vector, in beamforming the simplicity of the search process for the estimation of the sound speed is not affected and the *computational* problems introduced by nonlinearities are avoided.

The type of nonlinearity does affect the actual behaviour and the performance of the searching process; computational difficulties are present when a closed-form solution for the performances in the presence of modelling and estimation errors is sought, but not when the performance is evaluated by computer simulation.

8. – Observations on the array pre-processor

8˙1. *The* TC *and* CT *pre-processors.* – Two methods to estimate a cross-spectral matrix exist, the Correlate-and-Transform (CT) pre-processor, indicated in sect. **4**, and the Transform-and-Correlate (TC) pre-processor, which today is by far the most commonly employed one.

We define the propagation delay T_p along the array; this is given by the time difference between the maximum and the minimum values of mode propagation delays, plus the array length divided by the sound speed.

Figure 4(a) shows a sampled data implementation of the Transform-and-Correlate pre-processor. The observation interval is partitioned in nonoverlapping subintervals of duration $1/B_b$, such that the condition $B_b T_p \ll 1$ holds; by doing so, after taking FT in each subinterval, a vector data (= *snapshot*) in each frequency bin has a quasi-CW structure, and the mode contributions are (quasi) mutually coherent. In each

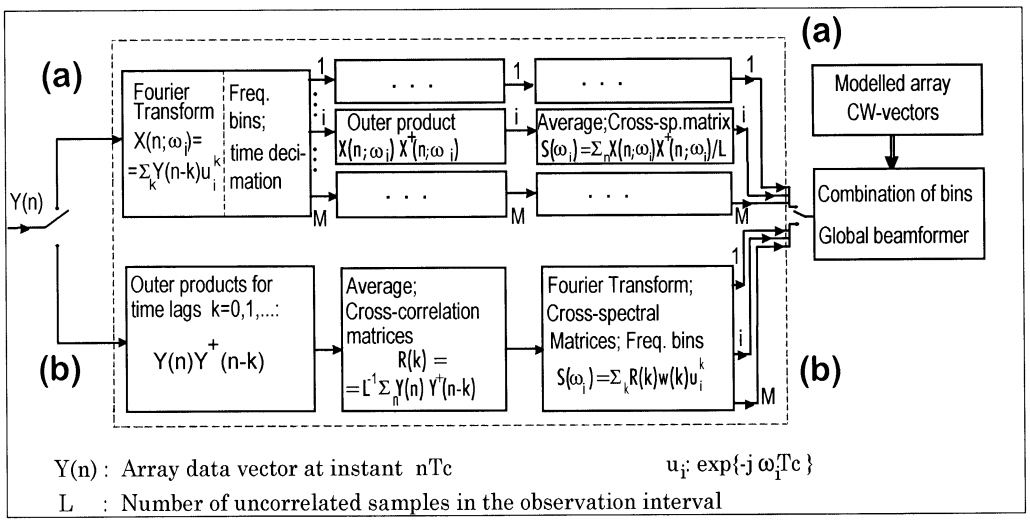

Fig. 4. – Estimating cross-spectral matrices from array data: (a) Transform-and-Correlate and (b) Correlate-and-Transform pre-processors.

sub-interval one outer vector product is computed for each bin, then time uncorrelated outer products, derived by distinct subintervals, are averaged bin per bin to obtain statistically stable estimates of $\mathbf{S}(\omega_i)$, the cross-spectral matrix for the i-th frequency bin. The channelisation of the array output data is performed to obtain cross-spectral matrices having nearly the same structural features valid for actual CW source signals so that the tomographic methods based on CW vector alignment criteria (eqs. (24), (27)) can be applied. The condition $B_b T_p \ll 1$ ensures that in each bin decorrelation along the array is negligible, and the cross-spectral matrix has a rank "nearly" equal to the number of sources.

Because a *modelled* array CW vector has a CW structure, employing an estimated cross-spectral matrix for beamforming tomography (eqs. (24), (27)) is fully motivated only when the matrix has the "right" outer product structure, which occurs exactly only for CW signals but not for finite-band signals. The matrix would achieve the required structure only asymptotically for $B_b \to 0$. Hence, in TC the problem of decorrelation along the array due to finite-band signals is only mitigated by dividing the bandwidth in frequency bins, but not eliminated.

The need of coping with array decorrelation is a serious constraint on the TC pre-processor: due to this constraint the duration of the subinterval may become unpractically large, depending on the array size, nonstationarity due to ship motion can impair the performance, etc.

Instead, the analysis in sect. **4** indicates that in the TC pre-processor no decorrelation problem arises, for any value of bandwidth: the cross-spectral matrix achieves the outer product structure required for beamforming exactly, for any value of source bandwidth.

Spectral estimation, which is an instrumental, intermediate step for the task of tomographic estimation, is introduced because the analysis of the time-dispersive channel is more convenient in the spectral domain, and to employ the body of methods

valid for CW signals in a wideband context. A requirement for tomography based on beamforming is that a cross-spectral matrix has the proper structure which is a weighted sum of outer products between array CW vectors relative to the sources.

The technique adopted in TC to fulfil the requirement employs two steps: the first is obtaining quasi-CW vector data (= snapshots) by dividing the wideband in frequency bins, the second is estimating the bin cross-spectral matrices. As a consequence of the first step, which is not a requirement from beamforming but it is instrumental to the second step, the matrices quasi-achieve the required structure. The TC processing criterion is sufficient but not necessary in order that the estimated cross-spectral matrices (quasi-) achieve the required structure. In fact, a requirement arises from beamforming only for the cross-spectral matrix structures, but not for the structures of the bin data after FT.

The CT technique consists in the search of a functional transform of the cross-correlation matrix $\mathbf{R}(\tau)$ able to generate cross-spectral matrices with the proper outer product structures, and it turns out that this functional transform is a FT. In the case of wideband and for a generic source-array scenario only the cross-spectral matrix and not the cross-correlation matrix $\mathbf{R}(\tau)$ has the required outer product structure. In CT it is not necessary to obtain CW or quasi-CW *data* as an intermediate step for beamforming.

The two pre-processors are shown in a discrete implementation in fig. 4(a) and (b). An amplitude tapering window $w(\tau)$ is introduced for the CT pre-processor [12, 24] which is zero for $|\tau| > \tau_0$, to minimise the estimation errors. The two pre-processors perform the same operations, but not in the same sequence. The operations are

– estimating the cross-correlation terms: computing elementary outer products and time averaging of the products to obtain matrix estimates,

– Fourier transform.

Although the operations are the same, the pre-processors are not identical: an outer product is a non-linear operation, so changing the operation sequence changes the result.

The TC and CT pre-processors are generalisations to arrays of two scalar estimates of the spectral power density of a stochastic process: a) the Periodogram, and b) the Blackman-Tukey spectral estimator (see [25], sect. **14**·2). In most of the applications of wideband beamformers found in technical literature, the pre-processor employed is TC. Although a sampled data version of the CT pre-processor was introduced first in [24], p. 1513, it does not seem that its properties have been fully recognised.

8·2. *The* CT *pre-processor and the Laplace transform*. – Examine the third member of eq. (13). Since the terms of the cross-correlation matrix decay to zero when the value of $|\tau|$ is sufficiently great, the two-sided Laplace Transform (LT) of the cross-correlation matrix can be considered, which may exist in a vertical strip of finite width in the p-plane (the LT variable is indicated by $p = \alpha + j\omega$) which includes the imaginary axis $j\omega$.

By performing the steps analogous to those indicated in eqs. (13) to (17) but for LT instead of FT, we derive easily

$$\mathbf{S}(p) = g_1(p)\, \mathbf{H}_1(p)\, \mathbf{H}_1^{+}(-p^{+}). \tag{44}$$

The points $(p, -p^{+})$ in the p-plane are symmetrical with respect to the imaginary

axis. Now the right and left array vectors can be derived by Singular Value Decomposition (SVD) of the cross-spectral matrix, apart from two phase-only scalar factors, which multiply all the components of the two vectors. An estimate similar to that in eq. (24) can be introduced

$$F(\Delta c) \equiv \frac{1}{1 - \frac{1}{M} \sum_{k=1}^{M} |\widetilde{\mathbf{H}}_1^+(p_k)\, \mathbf{H}_1(p_k)|^2} . \tag{45}$$

For the two-source case an estimator similar to that in eq. (27) can be introduced

$$F(\Delta c_1, \Delta c_2) \equiv \frac{1}{\sum_{k=1}^{M} |\widetilde{\mathbf{H}}_1^+(p_k)\, \mathbf{N}(p_k)\, \widetilde{\mathbf{H}}_1(-p_k^+) + \widetilde{\mathbf{H}}_2^+(p_k)\, \mathbf{N}(p_k)\, \widetilde{\mathbf{H}}_2(-p_k^+)|} . \tag{46}$$

If the LT exists in a strip of nonvanishing width in the p-plane, its introduction may be useful to increase the number M in the sums in eqs. (45), (46), by considering in the p-plane, beyond points for which $\alpha = 0$, also points where $\alpha \neq 0$. This might further decrease the likelihood of obtaining spurious estimates.

In the case of Laplace transform, the substitution $j\omega \rightarrow \alpha + j\omega$ induces another substitution in eq. (1) which defines the wavenumber

$$k^2(z) = \frac{\omega^2}{c^2(z)} \rightarrow -\frac{p^2}{c^2(z)} = \frac{\omega^2 - \alpha^2 - 2j\alpha\omega}{c^2(z)} . \tag{47}$$

This quantity has to be substituted in the Helmholtz equation (1), and also in eq. (4) which defines the depth eigen-functions; eq. (4) then becomes

$$\frac{\mathrm{d}^2\psi}{\mathrm{d}z^2} - (p^2 + \xi^2) = \frac{\mathrm{d}^2\psi}{\mathrm{d}z^2} + \left[\frac{\omega^2 - \alpha^2 - 2j\alpha\omega}{c^2(z)} - \xi^2 \right] \psi = 0 . \tag{48}$$

By assuming $\xi = \xi_r + j\xi_i$, we derive

$$\frac{\omega^2 - \alpha^2 - 2j\alpha\omega}{c^2(z)} - (\xi_r^2 - \xi_i^2 + 2j\xi_r\xi_i) = k_z^2 . \tag{49}$$

With respect to the case $\alpha = 0$, the quantity ξ in general will be a complex number, and not real and positive as in the case of $\alpha = 0$. Hence beyond a radial propagation term which is the complex exponential term in eq. (6), a radial attenuation (or amplification) factor, $\exp[-\alpha r]$, will be present.

To point out what occurs in a simple scenario, consider the case of a perfectly rigid bottom, with a value of c constant along the water column of depth H. The boundary condition at the bottom gives rise to the following constraint (see [26], sect. **12**·2.6, eq. (12.55)):

$$k_z H = \left(m - \frac{1}{2} \right) \pi , \qquad m = 1, 2, \ldots . \tag{50}$$

The dependence of the depth wavenumber k_z on the index m has been omitted in eq. (50). In this case the boundary condition at the bottom dictates that the value of k_z

does not change when passing from FT to LT (this may be not true in a scenario with a different type of bottom). Hence the following equation must hold:

$$\frac{\omega^2 - \alpha^2}{c^2} - (\xi_r^2 - \xi_i^2) = k_z^2, \qquad \frac{\alpha\omega}{c^2} + \xi_r \xi_i = 0 \,. \tag{51}$$

Hence

$$\frac{\omega^2 - \alpha^2}{c^2} - \left(\xi_r^2 - \frac{\alpha^2 \omega^2}{c^4} \frac{1}{\xi_r^2} \right) = k_z^2, \qquad \xi_i = - \frac{\alpha\omega}{c^2} \frac{1}{\xi_r} \,. \tag{52}$$

Equation (52) indicates that:

– The value ξ_r is modified with respect to the case $\alpha = 0$, but it is the same for $(p, \, -p^+)$.

– The value ξ_i changes sign when passing from p to $-p^+$.

Hence in this channel two modes (for $p, \, -p^+$) emerge for each index m, which are characterised, respectively, by exponential attenuation and by *amplification* with range.

The differential range attenuation between modes with distinct indices may be useful to highlight selectively certain modes with respect to others, giving extra freedom in the design of the tomographic estimators.

In the one-source case the vectors in eq. (45) can be chosen with exponential *attenuation* with range. In the two-source case left and right vectors in eq. (46) relative to the values $(p = \alpha + j\omega; \; -p^+ = -\alpha + j\omega)$ have not been sorted out from the noise subspace matrix $\mathbf{N}(p_k)$, so attenuating and amplifying modes are both present in the estimator. The presence of modes whose amplitude increases with range casts doubts on the applicability of estimators in which left and right vectors have not been sorted out as in eq. (45), and indicates that at most only small values of exponential amplification/attenuation on the whole channel could be applied. However, techniques exist to estimate left and right CW vectors so to employ only vectors with exponential attenuation in the estimators.

In spite of that, a practical difficulty still exists: when employing LT with $\alpha > 0$ instead of FT, in eq. (13) exponential attenuation occurs for $\tau > 0$, and magnification for $\tau < 0$. In the case of errorless estimation of $r_1(\tau)$ this function decays to zero rapidly enough for $|\tau| \to \infty$ to ensure the existence of LT in a nonvanishing strip in the p-plane. In practice errors arise when estimating $r_1(\tau)$ in a finite data interval. When applying LT the value of τ_0 beyond which the amplitude tapering function $w(\tau)$ (see fig. 4(b), [12, 24]) is zero should be increased with respect to FT due to the presence of the exponential magnification occurring for $\tau < 0$.

Note that when nearly CW vectors are obtained via TC technique (subsect. **7**˙1), nearly-CW signals are actually obtained at the frequency bin outputs and they are associated to the familiar CW waveguide modes. Instead, the modes emerging by LT with $\alpha \neq 0$, characterised by the exponential attenuation/amplification with range, do not correspond to modes which actually propagate, but they pop out from the particular signal processing adopted in the receiver, that is the decomposition of the cross-spectral matrix induced by LT.

9. – Conclusions

A new concept of tomography has been introduced, which employs passively the acoustic emission of ships of opportunity to estimate the environmental basin parameters. With respect to active tomography which employs *ad hoc* transmitters, the potential advantage of passive tomography is the absence of acoustic pollution, a simpler set-up as no transmitters are required, and perhaps the possibility of collecting significant amounts of data on a regular schedule.

A novel pre-processor has been described, which processes the wideband stochastic signals at the receiving array(s) output(s) to derive CW-like signals; then the same tomographic inversion algorithms valid for active tomography employing actual CW signals can be adopted to process the CW-like signals.

The potential advantages of the novel pre-processor, when compared with a more usually employed pre-processor, have been indicated.

With respect to active tomography, a loss of performances is likely to occur, due to a loss of observability of the channel introduced by passive techniques, and to the lack of knowledge of the emitted signals. It is conjectured that proper hardware/processing measures, such as increased array size and enhanced signal processing, can handle this problem.

To assess the performances of passive tomography, it would be useful to compare for the same propagation scenario an active system employing actual CW source signals and a passive system. As sea-collected data are available for active systems but not for the passive ones in which the source signals are different, it would be useful to compare the performances starting first from a simulated environment.

REFERENCES

[1] LEBRAS P., *Broadband modal filtering and array beamforming: application to modal tomography, Proceedings of the 2nd European Conference on Underwater Acoustics, Copenhagen, DK, July 1994*, edited by L. BJORNO (Tech. Univ. Denmark, for EC-DG XII) 1994, pp. 1089-1095.

[2] MUNK W. H. and WUNSH C., *Ocean acoustic tomography: rays and modes, Rev. Geophys. Space Phys.*, **21** (1983) 777-793.

[3] BAGGEROER A. B., KUPERMAN W. A. and MIKHALEVSKY P. N., *An overview of matched field methods in ocean acoustics, IEEE J. Ocean Engin.,* OE-**18** (1993) 401-424.

[4] BREKHOVSKIKH L. and LYSANOV Y., *Fundamentals of Ocean Acoustics* (Springer-Verlag, Berlin) 1982.

[5] Special Issue on *Detection and estimation in matched field processing, IEEE J. Ocean Engin.,* OE-**18** (3), July 1993.

[6] BUCKINGHAM M. J., *Ocean acoustic propagation models, J. Acoust.*, **3** (1992) 223-287.

[7] SHANG E. C. and WANG Y. Y., *Tomographic inversion of the El Niño profile by using a matched-mode processing (MMP) method, IEEE J. Ocean Engin.,* **19** (1994) 208-213.

[8] SCHUMACHER I. and HEARD G. J., *Removal of time-varying doppler using phase tracking with application to ocean warming measurements, J. Acoust. Soc. Am.*, **96** (1994) 1805-1820.

[9] HAWKER K. E., *A normal mode theory of acoustic doppler effects in the oceanic waveguide, J. Acoust. Soc. Am.*, **65** (1979) 675-681.

[10] CHEN H.-Y. and LU I.-T., *Matched mode processing schemes of a moving point source, J. Acoust. Soc. Am.*, **92** (1992) 2039-2050.

[11] ZALA C. and OZARD J. M., *Matched field processing for a moving source, J. Acoust. Soc. Am.*, **92** (1992) 403-417.
[12] GASPARINI O. and CAMPOREALE C., *Preliminary comparison between two spectral array pre-processors for wideband beamforming, Proceedings of IEEE Conference on Acoustic Speech and Signal Processing* (*ICASSP'95*), *May 1995, Detroit, MI* (Signal Processing Society of IEEE) 1995, pp. 3551-3555.
[13] SHANG E. C., *Ocean acoustic tomography based on adiabatic mode theory, J. Acoust. Soc. Am.*, **85** (1989) 1531-1537.
[14] WANG H. and KAVEH M., *Coherent signal subspace processing for the detection and estimation of angles of arrival of multiple wideband sources, IEEE Trans. on ASSP*, **33** (1985) 823-831.
[15] COLLINS M. D. and KUPERMAN W. A., *Focalization: environmental focusing and source localization*, *J. Acoust. Soc. Am.*, **90** (1991) 1410-1422.
[16] FEYNMAN R., *Lectures on Physics,* Vol. **1** (Addison Wesley, New York) 1965, eq. (34.4).
[17] TAROUDAKIS M. I., *A Comparison of the modal phase and modal travel time approaches for ocean acoustic tomography, Proceedings of the 2nd European Conference on Underwater Acoustics, Copenhagen, DK, July 1994*, edited by L. BJORNO (Tech. Univ. Denmark, for EC-DG XII) 1994, pp. 1057-1062.
[18] LYNCH J. F. *et al.*, *Acoustic travel time perturbations due to shallow water internal waves and internal tides in the Barents sea polar front: theory and experiment, J. Acoust. Soc. Am.*, **99** (1996) 803-821.
[19] TRAYKOVSKI P., *Travel time perturbations due to internal waves: equivalence of modal and ray solution, J. Acoust. Soc. Am.*, **99** (1996) 822-830.
[20] YANG T. C., *A method of range and depth estimation by modal decomposition, J. Acoust. Soc. Am.*, **82** (1987) 1736-1745.
[21] BOGART C. W. and YANG T. C., *Comparative performance of matched mode and matched field localization in a range-dependent environment, J. Acoust. Soc. Am.*, **92** (1992) 2051-2068.
[22] YANG T. C., *Effectiveness of mode filtering: a comparison of matched field and matched mode processing, J. Acoust. Soc. Am.*, **87** (1990) 2072-84.
[23] JESUS C. M., *Normal mode matching localization in shallow water: environmental and system effects, J. Acoust. Soc. Am.*, **90** (1991) 2034-2041.
[24] SU G. and MORF M., *The signal subspace approach for multiple wideband emitter location, IEEE Trans. on ASSP,* **31** (1983) 1502-1522.
[25] PAPOULIS A., *Probability, Random Variables and Stochastic Processes* (McGraw-Hill) 1984.
[26] BREKHOVSKIKH L. and GONCHAROV V., *Mechanics of Continua and Wave Dynamics* (Springer-Verlag, Berlin) 1985.